DESIGN OF FARMLAND AREA MEASURING INSTRUMENT BASED ON BEIDOU SATELLITE NAVIGATION SYSTEM
/
基于北斗导航系统的农田面积测量仪设计

Liang ZHANG [1 2], Ming LI [2], Limin YAO [3], Jingxin XIE [1], Xu XIAO [1] Jingjing HUANG [2], Jinqi HUANG [2], Xumeng LI [1], Kui FANG *[1]
[1]College of Mechanical and Electrical Engineering, Hunan Agricultural University, Hunan, 410125 / China;
[2]Hunan Agricultural Equipment Research Institute, Hunan Academy of Agricultural Sciences, Hunan, 410125 / China;
[3] College of Agricultural Engineering and Food Science, Shandong University of Technology, Shandong, 255000 / China
Tel: 18810987071; E-mail: 18810987071@163.com
DOI: https://doi.org/10.35633/inmateh-68-10

Keywords: *BeiDou Navigation Satellite System, farmland area, measuring instrument, triangulation*

ABSTRACT

Farmland area data is one of the important agricultural basic data, which provides parameter basis for the precise operation of agricultural equipment. In order to meet the technical needs of farmers and agricultural machinery operation service billing for acquiring basic information of farmland, this study proposes a farmland area measuring instrument based on the BeiDou Navigation Satellite System. Firstly, the overall design scheme of the measuring instrument, the hardware circuit design scheme and the algorithm design scheme are introduced, and the triangulation area measurement algorithm is emphatically analysed. Finally, the design of this research is applied. The farmland area measuring instrument measures the area of different shapes of farmland and verifies the measurement accuracy. The results show that the average relative error of the measuring instrument for measuring the area of irregularly shaped farmland is 0.7%, which realizes the rapid and high-precision measurement of the area of arbitrarily shaped farmland. It is hoped that this study can provide some reference for the research on the area measurement of farmland in my country.

摘要

农田面积数据是重要的农业基础数据之一，为农业装备实现精准作业提供参数依据。为满足农户和农机作业服务计费等市场对获取农田基本信息的技术需要，本研究提出一种基于北斗卫星导航系统的农田面积测量仪。首先，介绍了测量仪的总体设计方案，硬件电路设计方案和算法设计方案，着重分析了三角剖分面积测量算法设计。最后，应用了本研究的设计。农田面积测量仪测量测量不同形状农田的面积，并验证测量精度。结果表明，测量仪对不规则形状农田面积测量的平均相对误差为 0.7%，实现对任意形状农田面积的快速高精度测量。希望这项研究能为我国农田的面积测量研究提供一定的参考。

INTRODUCTION

Agricultural information technology is the main direction of the development of modern agriculture (*Poppe K. J. et al., 2013*). Farmland area data is an important agricultural basic data *(Yuefeng Du et al, 2019*). Farmland area data provides the basis for agricultural equipment to achieve precise operations, such as precision ploughing, precise fertilization, precise irrigation and precise harvesting *(Xuegeng Chen et al, 2020*).

The current domestic and international farmland area measurement mainly includes:

(1) The tape measure method is only applicable to regular and small-area farmland.

(2) The professional instrument measurement method (total station, etc.) requires professional and skilled operators, complicated calculation, high cost, and is not suitable for farmland area measurement.

(3) The area measuring instruments based on the satellite navigation system are widely used in agriculture (*Dengsheng Zhu et al, 2020*). Researchers at home and abroad have studied the vehicle-mounted farmland area measuring instrument, which calculates the farmland area by recording the length of the track of farm machinery operation and the width of the operation through GNSS (Global Navigation Satellite Systems, GNSS) positioning module/GNSS and AHRS integrated system (*Yunpeng Jing et al, 2019*), but there are errors such as operation track overlap or omission, and the measurement error increases with the increase of operation overlap area or omission;

Yangchun Liu et al. used the third method mentioned above to obtain the farmland area by multiplying the length of the operating trajectory with the width. Because of the overlapping trajectories during the operation, the measured area was larger than the true value, and the experiment showed that the error between the area calculated by this method and the area measured by the tape was generally stable within 3%, which increases with the increase of overlapping trajectories (*Yangchun Liu et al, 2016*).

Binbin Ji et al. used GPS (Global Positioning System, GPS) to measure the trajectory length of agricultural machinery, and used ultrasonic sensors to measure the width of agricultural machinery, and multiplied the trajectory length and width to measure the area of farm machinery operations in real time, and the average error between the area obtained by the device and the actual area was less than 2% (*Binbin Ji et al, 2012*).

Zhixiong Lu et al. used a dual-satellite positioning receiver of GPS and Galileo to improve the positioning accuracy by adaptive filtering algorithm. The area was calculated using the multiplication of track length and width, and the relative error of area measurement was 2.09% (*Zhixiong Lu et al, 2015*).

Hui Liu et al. designed vector buffer algorithm and raster buffer algorithm for agricultural machine operation area measurement, and conducted experiments under three different GNSS positioning accuracy conditions of RTK (Real-Time Kinematic Positioning, RTK), sub-meter level and single-point positioning, respectively and the results showed that GNSS positioning accuracy had significant effects on operation area measurement accuracy. The relative measurement errors of the two algorithms were 0.31% and 0.18%, when RTK positioning was used; 2.43% and 1.44% when sub-meter GNSS positioning was used; 7.20% and 6.31% when single-point GNSS positioning was used. The area measurement accuracy decreases with the decrease of GNSS positioning accuracy (*Hui Liu et al, 2015*).

Researchers at home and abroad have studied handheld farmland area measuring instruments, which measured the coordinates of farmland boundary points and sequentially connected them to obtain farmland areas through the positioning function of GPS. *Zhengjun Qiu et al.* used the GPS positioning function to develop a measuring instrument for farmland area. The farmland area measuring instrument consists of GPS module, microcontroller, keyboard and LCD display, and adopts GPS positioning technology and polygonal farmland area calculation method. The results showed that the measuring instrument can quickly measure the area of farmland the relative error less than 2% (*Zhengjun Qiu et al, 2005*). In this measurement method, the measurement accuracy of the boundary point and distance between the two measurement points will affect the shape of the measurement fitting graph. The closer to the actual farmland, the smaller the measurement error (*Yizhe Sun et al, 2019*). Therefore, the improvement of the boundary point measurement accuracy and the improvement of the shape fitting method will improve the measurement accuracy of farmland area. To sum up, the farmland area measuring instrument has problems such as large overlapping error of measuring area, low accuracy of boundary point measurement, and the farmland shape fitting method needs to be improved.

With the construction of BeiDou Navigation Satellite System ground-based augmentation stations and the development of mobile communication technology (*Guangqi Wang et al, 2018*), high-precision navigation and positioning services were provided (*Sunwen Li et al, 2021*). Triangle is the smallest unit to calculate polygon area, which can be closer to polygon boundary (*Gopi M. et al, 2000*). In this paper, we adopt the BeiDou network differential technology to improve the positioning accuracy of the area measuring instrument, and combined the triangular dissection algorithm to improve the accuracy of polygonal farmland area measurement and eliminate the overlapping error. The hardware design of the farmland area measuring instrument was completed by embedded technology to realize convenient measurement of the area of any shaped farmland.

MATERIALS AND METHODS

The overall design of the farmland area measuring instrument system

The farmland area measuring instrument is mainly composed of BeiDou high-precision positioning module, communication module, Raspberry Pi, HDMI display, power module and virtual keyboard, as shown in Figure 1. The Raspberry Pi is used as the main control board of the farmland area measuring instrument. It is equipped with a 1.2 GHz quad-core Broadcom BCN2837 64-bit ARMv8 processor, and integrates 4 USB2.0 ports and a 40-pin extended GPIO interface. The main control board transmits data through the communication module and the BeiDou high-precision positioning module, collects the latitude and longitude coordinates of the farmland boundary points, and uses the triangulation farmland area calculation algorithm to measure and display the farmland area.

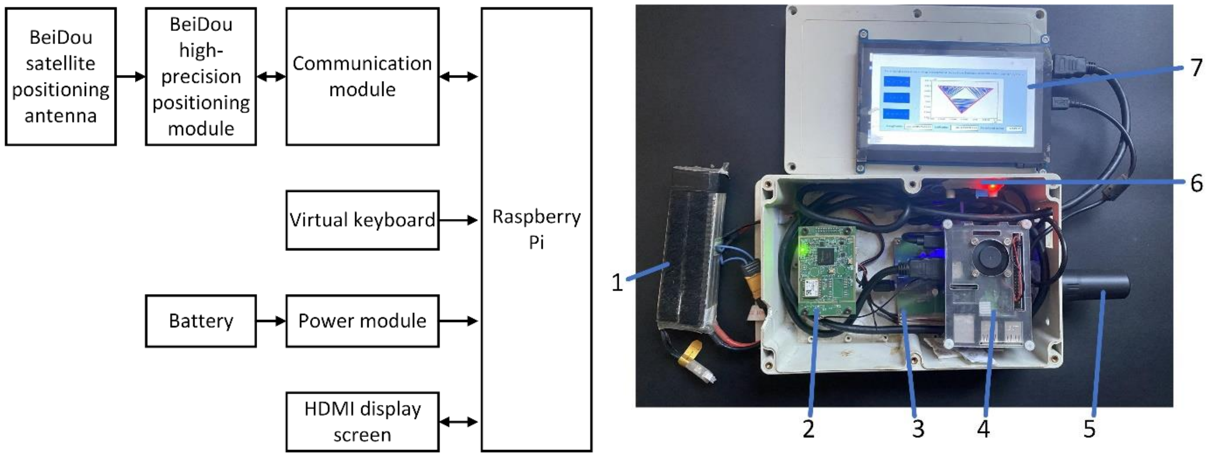

Fig. 1 –General structure of farmland area measuring instrument design
1-Battery; 2-BeiDou high-precision positioning module; 3-Power module; 4-Raspberry Pi;
5-BeiDou satellite positioning antenna; 6-Communication module; 7-HDMI display screen

Hardware design of farmland area measuring instrument

As shown in Figure 2, the farmland area measuring instrument collects the latitude and longitude coordinates of the farmland boundary points, and the positioning error of the boundary points will affect the accuracy of area measurement. Because the MC120M module integrates the single-frequency RTK algorithm, and supports both BeiDou satellite navigation system and the global satellite navigation system, the data update frequency is 1 Hz, the positioning accuracy of MC120M module can reach real-time centimetre level. Therefore, the MC120M is chosen for its accurate positioning, ease of use and low cost. The MC120M module has two power input pins (VCC, V_BACKP) and one power output pin (VCC_RF). The VCC pin is connected to the positive pole of 3.3V power supply, and the GND pin is connected to the negative pole of the power supply to supply power to the module; The V_BCKP pin is connected to 3.3V backup power supply to power the RTC circuit when VCC power failure occurs to ensure the critical information is not lost for hot start function; VCC_RF outputs 3.0V voltage, which can be used to power the antenna; The RF_IN pin is the antenna interface of the module, with built-in 50 ohm impedance matching, which can be directly connected to the multimode antenna; The module comes with its own internal power-on reset circuit, so the RESET_N reset pin is overhung; The TIMEPULSE pin is the second pulse signal output, which is output after several seconds after the module obtains the positioning data, and is used to indicate the positioning status. Therefore, the TIMEPULSE pin is connected to the LED for displaying the positioning status. The TXD and RXD pins are the UART serial port pins of the module, which are respectively connected to the RXD and TXD pins of the communication module, used to communicate with the main control board, and the supported baud rate range is 4800 bps ~ 460800 bps. At startup, the D_SEL pin of the module controls the type of data interface used for communication. When this pin is high or overhung, the UART protocol is chosen. When this pin is low, the SPI protocol is chosen. The UART protocol is selected, so D_SEL is designed to be overhung, and the circuit design is shown in Figure 3.

Fig. 2 - The photos of the operation of collecting the coordinates of the experimental farmland to be measured

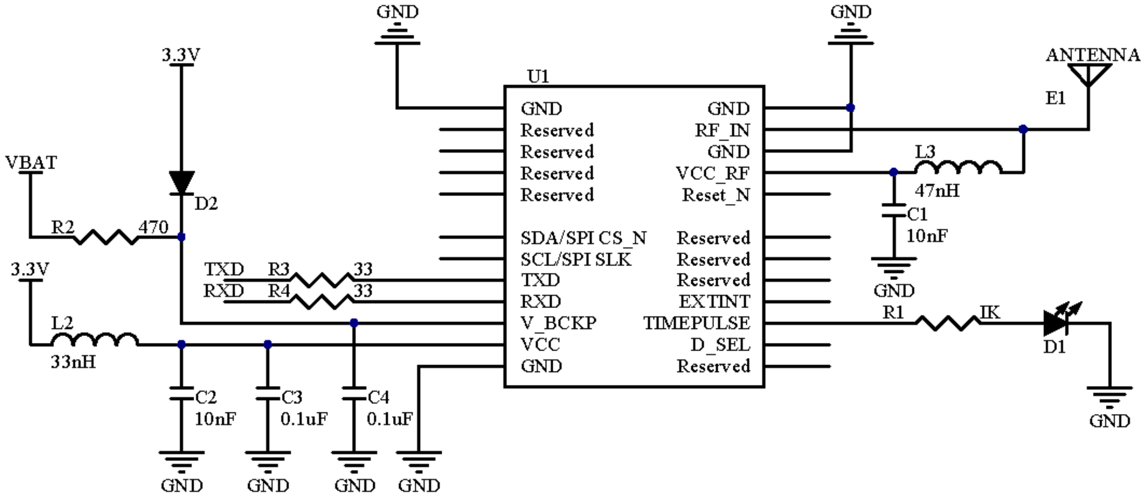

Fig. 3– Design of BeiDou high-precision positioning module circuit of the system

In order to realize the data exchange between the BeiDou high-precision positioning module and the Raspberry Pi, the communication interface circuit of USB to serial port is designed. The CH340T is a USB bus adapter chip used to extend the serial port for the computer or upgrade the serial port devices directly to the USB bus, and it supports full-speed USB device interface and is compatible with USB V2.0. The external circuit components only require a crystal oscillator and capacitors, the circuit design is simple and stable, so the communication interface circuit adopts CH340T chip. The CH340T chip has a built-in USB pull-up resistor, and the UD+ and UD- pins can be connected directly to the USB bus. The clock signal is generated by the built-in inverter through the crystal oscillator frequency stabilization oscillator, so a 12 MHz crystal oscillator is connected between pins XI and XO, and oscillating capacitors C5 and C6 are connected to ground for pins XI and XO, respectively. The CH340T chip supports 5V power supply voltage, VCC pin input external 5V power supply, and V3 pin is connected with power supply decoupling capacitors with capacities of 0.01 μF, 0.1 μF and 22 μF respectively. The data transmission pins TXD and RXD are respectively connected with the RXD and TXD of the MC120M module for data transmission and reception. The design of the communication interface circuit is shown in Figure 4.

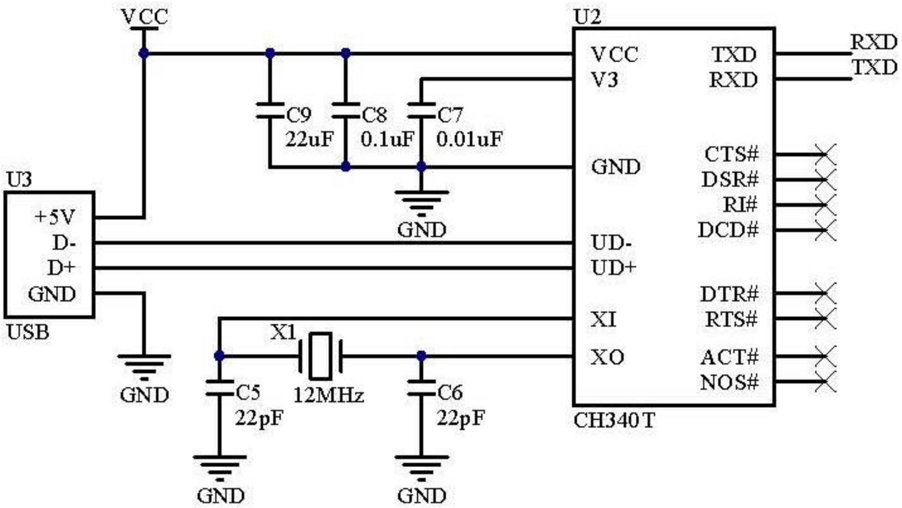

Fig. 4 – Design of communication interface circuit of the system

Algorithm design of farmland area measuring instrument

Using satellite positioning technology to measure the farmland boundary points, the area of the polygon enclosed by the boundary points is the farmland area. The measured farmland is flat dam farmland with a slope of 0° to 6° and suitable slope farmland with a slope of 6° to 25°. Triangle is the smallest unit to calculate polygon area, which can be closer to polygon boundary. The idea of micro-integration is adopted. Firstly, the undulating polygonal farmland is divided into many triangle areas, which are closer to the local terrain, and then the farmland area is obtained by accumulating the area of each small triangle. The more complex the shape of the farmland, the more undulating the ground, which makes it difficult for the triangle to approach the local terrain, reducing the accuracy of farmland area measurement. The Delaunay triangulation method was used to calculate the farmland area. First, the WGS84 (World Geodetic System (WGS) 1984) coordinate of the farmland boundary points were converted into the Local Cartesian coordinate system, and the discrete boundary points were connected into adjacent and non-overlapping triangles through Delaunay triangulation. The sum of the triangle area is the polygonal farmland area. The triangle can be closer to the complex boundary (The complex boundary composes of more than three lines on different planes that connect in sequence and do not intersect.). Compared with the boundary method, the figure formed by the triangulation algorithm is closer to the actual polygonal farmland, and the measurement error is smaller; compared with the traditional multiplication of width and trajectory, the triangulation algorithm forms adjacent and non-overlapping triangles without overlapping measurement areas. Therefore, the combination of high-precision positioning and Delaunay triangulation method will further improve the accuracy of the farmland area measuring instrument.

The surface of the earth is a curved surface. In order to accurately calculate the farmland area, Gauss projection positive operator is used to expand the curved surface into a plane, and the Krasovsky ellipsoid parameters are used for Gauss projection positive operator, and the WGS84 coordinates of the farmland boundary points are converted into the Local Cartesian coordinate system. Delaunay triangulation makes a finite set of points connected to each other to form a plane formed by a set of adjacent and non-overlapping triangles. Delaunay triangulation is performed on the boundary points of the farmland through the point-by-point interpolation method, and the farmland is divided into a plane formed by a set of triangles, and the area of the farmland is obtained by calculating the sum of triangle area.

The Gaussian coordinates of the boundary points are arranged according to the x and y values from small to large, and a rectangle is established with the points (x_{min}, y_{min}) and (x_{max}, y_{max}) as the diagonal. Based on the diagonal triangle of a half rectangle, the hypotenuse of a right triangle after doubling it according to the similar triangle theorem passes through the point (x_{max}, y_{max}). The base and height of the triangle are expanded, and the expansion principle always maintains that the length of the base of the expanded triangle is greater than the height. As shown in Figure 5, the expanded triangle is symmetrically copied into a triangle enclosing the Gauss coordinate points of the farmland boundary to determine the maximum distribution of the farmland.

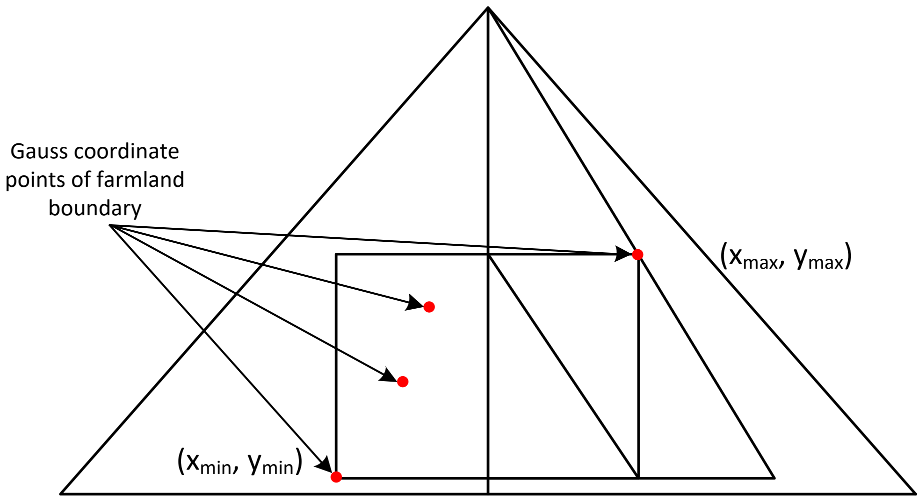

Fig. 5 – The triangle enveloping all points

The point-by-point interpolation to create a triangular mesh: The envelope triangle is put into the temporary triangle list, and the external circles are calculated one by one for the triangles in the temporary triangle list. First, we calculate the external circle of the envelope triangle, as shown in Figure 6. Then, the judgment is made one by one from the point with the x coordinate from small to large. It is found that any point is within the external circle of the enveloping triangle, so the enveloping triangle is not a Delaunay triangle. We save its three sides to the edge buffer array, and delete the enveloping triangle from the temporary triangle list.

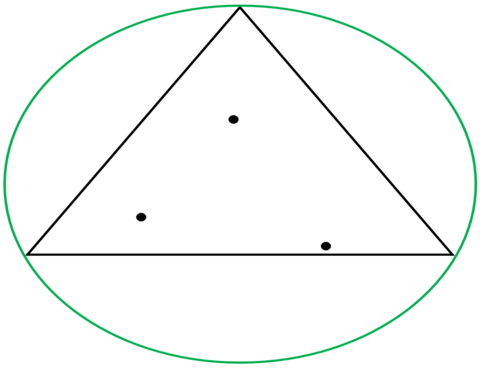

Fig. 6 – The circumscribed circle of enveloping triangle

In the sorted coordinate points, as shown in Figure 7, the point with the smallest x-coordinate value is connected to each edge in the edge buffer array to form three triangles, and the formed triangles are added to the temporary triangle list. As shown in Figure 8, the triangles in the temporary triangle list are traversed to draw the external circle, and the positional relationship between the external circle and the second-smallest point of the x-coordinate value is determined. If the point is on the right side of the circumcircle of the triangle, it means that the triangle is a Delaunay triangle, and the triangle is saved to the list of Delaunay triangles.

If the point is measured to the left of the external circle of the triangle, the triangle will not be judged this time, and it will not be deleted from the temporary triangle list, and the judgement will be made after the next coordinate point is inserted; If the point is inside the external circle of the triangle, the three sides of the triangle are added to the edge buffer array. The point continues to form a triangle with the edge in the edge buffer array and put it in the temporary triangle list, and traverse the positional relationship between each triangle external circle and the next insertion point in the temporary triangle list. All the coordinate points are gradually inserted, and the judgment is carried out in turn. Finally, the triangles related to the three points of the envelope triangle are removed from the list of Delaunay triangles, and the remaining triangles are the triangles formed by the division. As shown in Figure 9, a piece of farmland on the satellite map is divided into many small triangles.

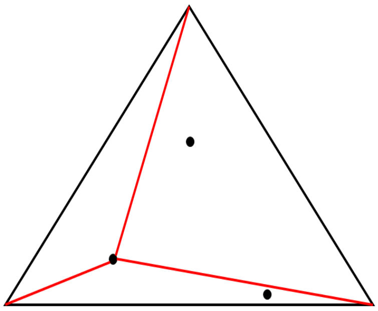

Fig. 7 – The triangles formed by the point inside the triangle and the three sides of the triangle

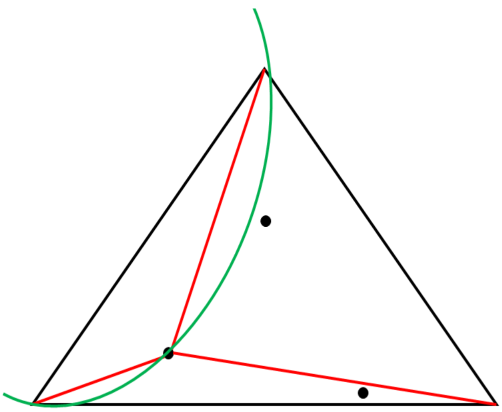

Fig. 8 – The external circle of triangle

Fig. 9 –The Delaunay triangulation of farmland

The calculation of polygonal farmland area: After the division, the side length of each small triangle is obtained, and the area of each small triangle after division is obtained by Heron formula, and the total area of the farmland is obtained by summing the areas of the divided triangles.

$$S_i = \sqrt{p_i\big((p_i - a_i)(p_i - b_i)(p_i - c_i)\big)} \quad (1)$$

Where:

S_i is the area of the small triangle. a_i,b_i,c_i are the lengths of the three sides of the small triangle. p_i is the semiperimeter.

$$S = \sum S_i \quad (2)$$

Where: S is the farmland area.

Software design of farmland area measuring instrument

The program adopts modular design to meet the portability of the program. Each functional program includes: BeiDou information collection module, area calculation module, display module and storage module. The flow chart of the program is shown in Figure 10. The BeiDou information collection module reads the positioning information and judges whether the measurement starts. At the beginning of the measurement, the integrity of the positioning information is judged. The latitude and longitude data is obtained and stored by calculating the difference correction number and the original positioning data. When the device measurement is complete, the triangulation area algorithm is run.

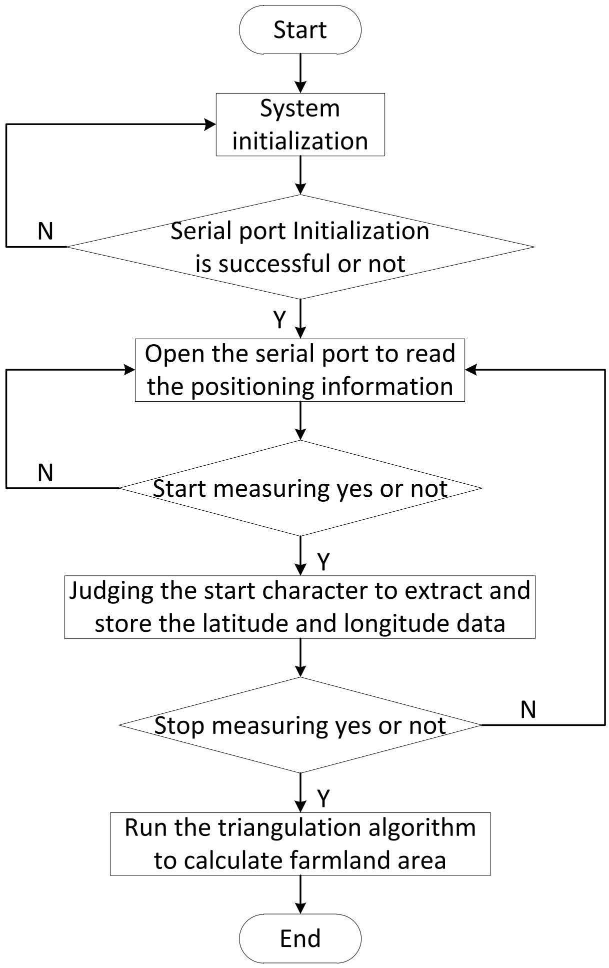

Fig. 10 – The program flow chart of system

After opening the desktop application, click the “measure button” to complete the initialization of the serial port and the BeiDou high-precision positioning module, and then display the differentially calculated high-precision positioning data below the desktop application, as shown in Figure 11.

Then the area measuring instrument starts measuring. When the measurement is finished, click the “End Measurement” button. The triangulation area algorithm implements the area calculation and displays the triangulation map.

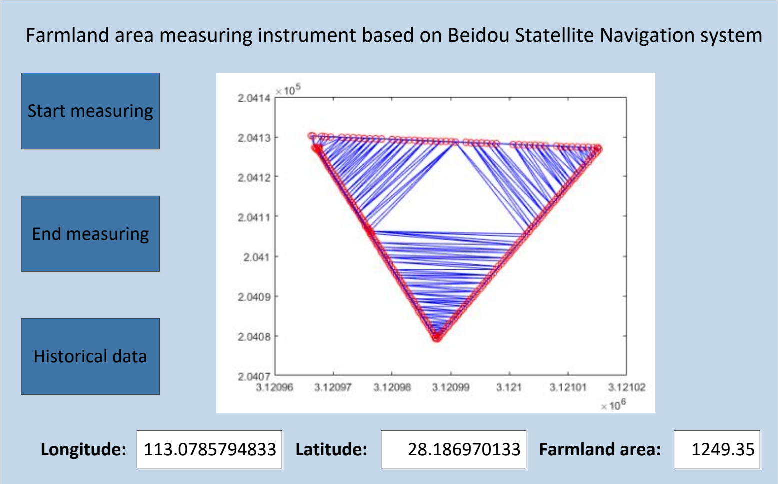

Fig. 11 – The software interface of farmland area measuring instrument

RESULTS

The experimental design of farmland area measurement

In October 2021, the measurement accuracy experiment of the farmland area measuring instrument was carried out in the farmland of Hunan Agricultural Equipment Research Institute near Hunan Agricultural University. The experiment selects square, rectangular, triangular, circular and polygonal plots as the experiment site. The measuring area of the tape is the standard area of the experiment site. The standard areas of the five shape experiment sites (as shown in Figure 12) are: the area of the ABCD square $S_1 = AB \times BC = 50\,m \times 50\,m = 2500\,m^2$; the area of the ABGE rectangular $S_2 = AB \times BG = 50\,m \times 25\,m = 1250\,m^2$; the area of the EBC triangle $S_3 = 0.5 \times EG \times BC = 0.5 \times 50\,m \times 50\,m = 1250\,m^2$; the area of the EFGH circular $S_4 = 3.14 \times\ OF \times OF = 3.14 \times 25\,m \times 25\,m = 1962.5\,m^2$; the area of the FKCIE polygon $S_5 = 781.25\,m^2 + 468.75\,m^2 + 312.5\,m^2 = 1562.5\,m^2$. The hand-held farmland area measuring instrument walks around the boundary of the experiment site to obtain the field measurement area, and the walking speed is about 1 m/s, and the experiment is repeated five times for each experiment site.

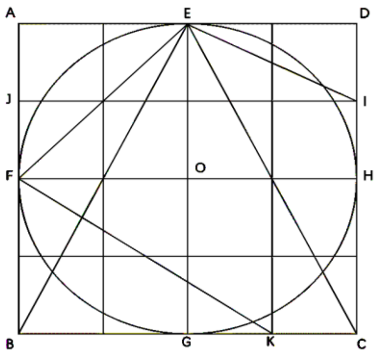

Fig. 12 – The experiment area

Experimental results and analysis

Table 1 shows the data processing results of the standard area, measurement area and relative error of the experiment plot. Figure 13 is the GIS map of the ABEG experimental farmland. Figure 14 is a measurement diagram processed by a triangulation area measurement algorithm. When measuring square, rectangular and circular experiment sites, due to the regular shape, small number of vertices and no sharp vertices, the set of boundary points obtained by the farmland area measuring instrument is accurate, and the average error is 0.5%, 0.516% and 0.556% respectively. When measuring the polygon experimental farmland, due to the irregular shape and many vertices, the boundary points obtained by the farmland area measuring instrument near the polygon vertices are lost. With the increase of polygon vertices the loss of boundary points increases and the average error reaches a maximum of 0.998%. When measuring the triangle experimental farmland, the three vertex angles are all acute angles, the boundary points obtained by the farmland area measuring instrument at the vertex angles are seriously lost, and the average measurement error reaches 0.924%.

Table 1

Comparison of test results of farmland area measuring instrument

Region	Standard area (m^2)	Measurement number	Instrument measurement (m^2)	Difference (m^2)	Relative error (%)	Average relative error (%)
square	2500	1	2498.39	1.61	0.06	0.500
		2	2507.06	7.06	0.28	
		3	2531.64	31.64	1.27	
		4	2486.27	13.73	0.55	
		5	2491.62	8.38	0.34	
rectangular	1250	1	1262.33	12.33	0.99	0.516
		2	1242.37	7.63	0.61	
		3	1245.78	4.22	0.34	
		4	1257.49	7.49	0.60	
		5	1249.50	0.5	0.04	
triangle	1250	1	1279.84	29.84	2.39	0.924
		2	1249.35	0.65	0.05	
		3	1241.61	8.39	0.67	
		4	1258.31	8.31	0.66	
		5	1260.57	10.57	0.85	
circular	1962.5	1	1968.02	5.52	0.28	0.556
		2	1975.47	12.97	0.66	
		3	1972.95	10.45	0.53	
		4	1981.36	18.86	0.96	
		5	1969.40	6.90	0.35	
polygon	1562.5	1	1584.71	22.21	1.42	0.998
		2	1560.48	2.02	0.13	
		3	1568.87	6.37	0.41	
		4	1596.84	34.34	2.20	
		5	1575.45	12.95	0.83	

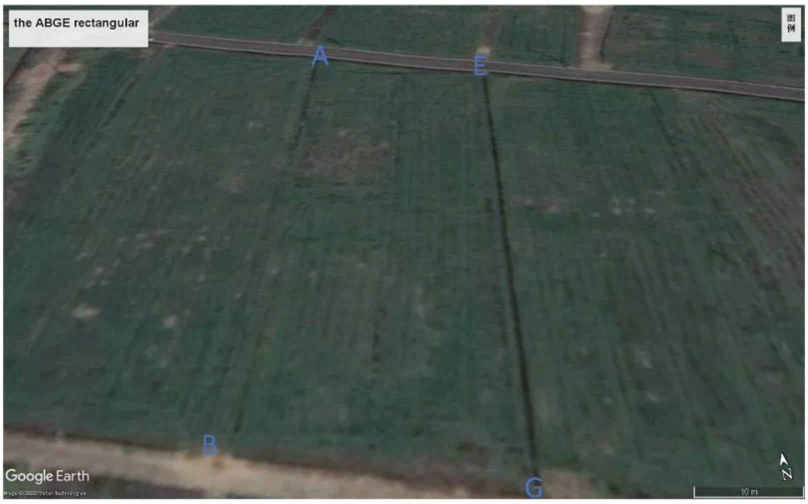

Fig. 13 – The GIS map of the ABEG experimental farmland

The experiment results show that the farmland area measuring instrument can accurately measure the farmland area regardless of the shape of the farmland, and the average error rate of the measurement area is maintained below 0.7%. When measuring polygons with multiple sharp vertices, the measurement error rate increases, and the maximum measurement error does not exceed 2.5, which fully meets the needs of farmland area measurement.

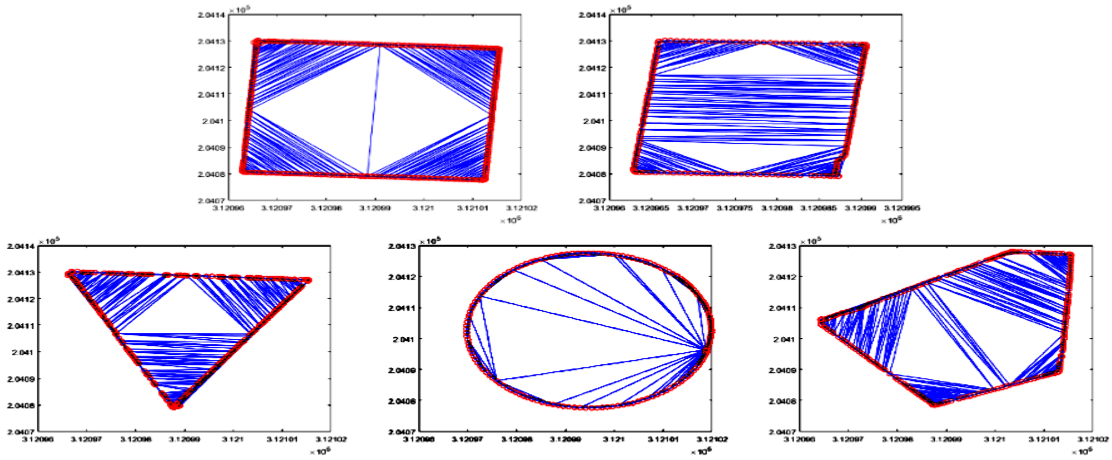

Fig. 14– The area measurement map of farmland

CONCLUSIONS

Based on the BeiDou Navigation Satellite System, this research developed the BeiDou high-precision and communication interface circuit, designed the triangulation farmland area measurement algorithm, and applied the algorithm to the software development of the farmland area measuring instrument. In the area measurement of small-scale farmland, the farmland area measuring instrument based on the BeiDou Navigation Satellite System can accurately measure the farmland area regardless of the shape of the farmland, and the average error of the measurement area is maintained below 0.7%. When the farmland area measuring instrument measures acute-angled triangles and polygonal plots, the measurement error increases, but the measurement does not exceed 2.5%, and the measurement accuracy is significantly improved, which meets the requirements of farmland area measurement. There are also some shortcomings in this study. When measuring the boundary of the plot with acute angle vertices, the measured boundary points at the vertices are seriously lost. In order to reduce the measurement error, in future research, the data update frequency of the BeiDou high-precision positioning module will be increased.

ACKNOWLEDGEMENT

The authors greatly appreciate the careful and precise reviews by anonymous reviews and editors. The study was supported by “Natural Science Foundation of Hunan Province (Grant No.2021JJ40287)” and “Changsha Natural Science Foundation (Grant No.kq2014174)”.

REFERENCES

[1] Binbin Ji, Jun Li, Yuping Yang, Sen Zhang, (2012), A real-time measurement based on GPS which was designed for calculating the harvest area of combine. *Chinese Agricultural Mechanization*, Vol.244, no.6, pp.89-92, China;

[2] Dengsheng Zhu, Hui Fang, Shaoming Hu, Wenquan Wang, Yansuo Zhou, Hongyan Wang, Fei Liu, Yong He, (2020). Development and Application of an Intelligent Remote Management Platform for Agricultural Machinery. *Smart Agriculture*, Vol.2, no.2, pp.67-81, China;

[3] Gopi M., Krishnan S., Silva C.T., (2000), Surface Reconstruction based on Lower Dimensional Localized Delaunay Triangulation. *Eurographics*, Vol.19, no.3, Blackwell Publishers Ltd, Britain, pp.467-478;

[4] Guangqi Wang, Yu Han, Jian Chen, Shubo Wang, Zichao Zhang, Nannan Du, Yongjun Zheng, (2018), A GNSS/INS Integrated Navigation Algorithm Based on Kalman Filter. *IFAC-PapersOnLine*, Vol.51, no.17, Elsevier, Netherlands, pp.232-237;

[5] Hui Liu, Zhijun Meng, Weiqiang Fu, (2012), Overlap and skip evaluation for agricultural machinery operation based on GPS track logs. *Transactions of the Chinese Society of Agricultural Engineering*, Vol.28, no.18, pp.149-154, China;

[6] Hui Liu, Zhijun Meng, Pei Wang, Xueli Wei, Yu Han, (2015), Buffer algorithms for operation area measurement based on global navigation satellite system trajectories of agricultural machinery. *Transactions of the Chinese Society of Agricultural Engineering*, Vol.31, no.7, pp.180-184, China;

[7] Poppe K.J., Wolfert S., Verdouw C., Verwaart T., (2013), Information and Communication Technology as a Driver for Change in Agri-food Chains. *EuroChoices*, Vol.12, no.1, pp.60-65, Britain;

[8] Shuwen Li, Qianxin Wang, Wei Wu, (2021), Analysis of global positioning accuracy of BDS-3 single and dual frequency signals. *Science of Surveying and Mapping*, Vol.46, no.12, pp.67-74, China;

[9] Xuegeng Chen, Haojun Wen, Weirong Zhang, Fochu Pan, Yan Zhao, (2020), Advances and Progress of Agricultural Machinery and Sensing Technology Fusion. *Smart Agriculture*, Vol. 2, no.4, pp.1-16, China;

[10] Yangchun Liu, Yanwei Yuan, Junning Zhang, Fengzhu Wang, Kang Niu, (2016), Design and Experiment of Remote Management System for Subsoiler. *Transactions of the Chinese Society for Agricultural Machinery*, Vol.47, pp.43-48, China;

[11] Yizhe Sun, Ji Li, Bin Liu, Yu Xie, He Gong, (2019), Measurement of agricultural machinery operation area based on improved Alpha Shapes algorithm. *Journal of Chinese Agricultural Mechanization*, Vol.40, no.8, pp.144-148, China;

[12] Yuefeng Du, Shenghui Fu, Enrong Mao, Zhongxiang Zhu, Zhen Li, (2019), Development Situation and Prospects of Intelligent Design for Agricultural Machinery, *Transactions of the Chinese Society for Agricultural Machinery*. Vol.50, no.9, pp.1-17, China;

[13] Yunpeng Jing, Gang Liu, Zhikun Jin, (2019), Topographic survey of farmland based on GNSS dual antenna combined with AHRS. *Transactions of the Chinese Society of Agricultural Engineering*, Vol.35, no.21, pp.166-174, China;

[14] Zhengjun Qiu, Xiafang Ying, Yong He, (2005). A portable instrument for measuring field area based on GPS module. *Journal of Zhejiang University*, Vol.31, no.3, pp.333-336, China;

[15] Zhixiong Lu, Wenjun Zhong, Xiuyong Diao, Shikun Mei, Jing Zhou, Zhun Cheng, (2015), Measurement of field area based on tractor operation trajectory. *Transactions of the Chinese Society of Agricultural Engineering*, Vol.31, no.19, pp.169-176, China.